Electronic Supplementary Information

Strain-Tunable Spin Filtering and Valley Splitting Coexisting with Anomalous Hall Effect in 2D Half-Metallic VSe_2/VN Heterostructure: Toward a Unified Spintronic-Valleytronic Platform

Vivek Chowdhury [1], Ahmed Zubair [1,*]

[1]Department of Electrical and Electronic Engineering, Bangladesh University of Engineering and Technology, Dhaka 1205, Bangladesh

[*]Corresponding author: ahmedzubair@eee.buet.ac.bd

S1. Band Structure (with SOC) and Work Function of Pristine Hexagonal VSe_2 Monolayer

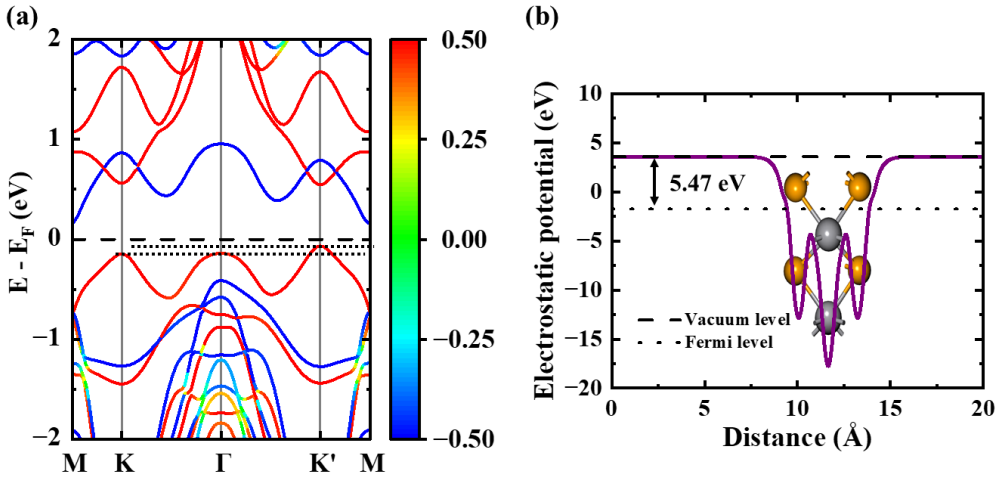

Fig. S1: Band structure and work function of monolayer hexagonal VSe_2. (a) Band structure (with SOC) of monolayer hexagonal VSe_2. The dotted lines indicate valley splitting, and the color map indicates expectation values of the spin operator on the spinor wave-functions, ranging from -0.50 (blue) to +0.50 (red). (b) Work function plot showing vacuum and Fermi level of monolayer hexagonal VSe_2.

Figs. S1(a) and (b) illustrate the spin–orbit coupling (SOC) induced band structure and work function of monolayer VSe_2. A valence band valley splitting of 79.2 meV was observed at the K and K′ points, along with an indirect band gap of 0.29 eV obtained using the PBE functional. The conduction band minimum and valence band maximum were found at the M and K′ points, respectively. These results are in excellent agreement with previously reported values of 78 meV for valley splitting and 0.28 eV for the band gap [1]. The calculated work function also aligns closely with the value of 5.51 eV reported in a previous study [2].

S2. Band Structure(with SOC) and Work Function of Pristine Hexagonal VN Monolayer

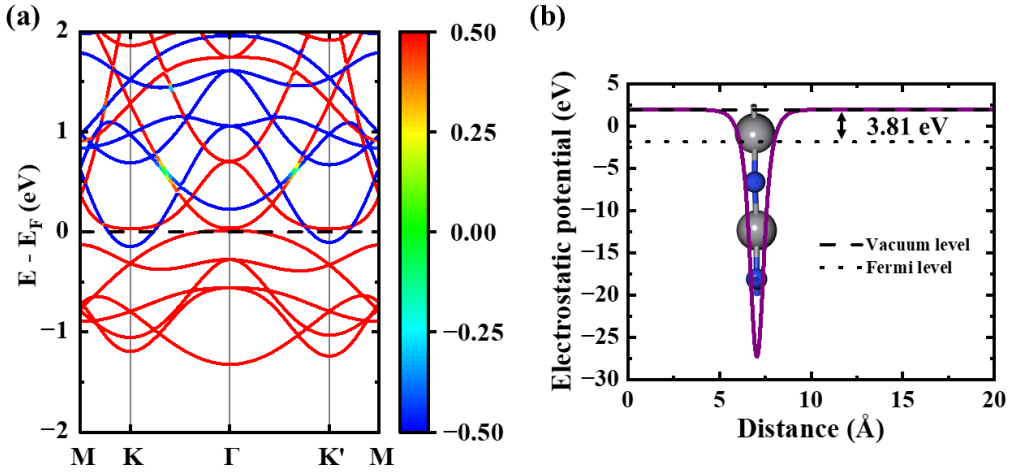

Fig. S2: Band structure and work function of monolayer hexagonal VN. (a) Band structure (with SOC) of monolayer hexagonal VN. The color map indicates expectation values of the spin operator on the spinor wave-functions ranging from -0.50 (blue) to +0.50 (red). (b) Work function plot showing vacuum and Fermi level of monolayer hexagonal VN.

Figs. S2(a) and (b) present the SOC induced band structure and work function of monolayer hexagonal VN. The metallic character observed in the band structure is consistent with previously reported results [3]. Additionally, the calculated work function shows good agreement with the previously reported value of 3.776 eV [4].

S3. Effect of Strain in Spin Density Diagram in VSe_2/VN Heterostructure

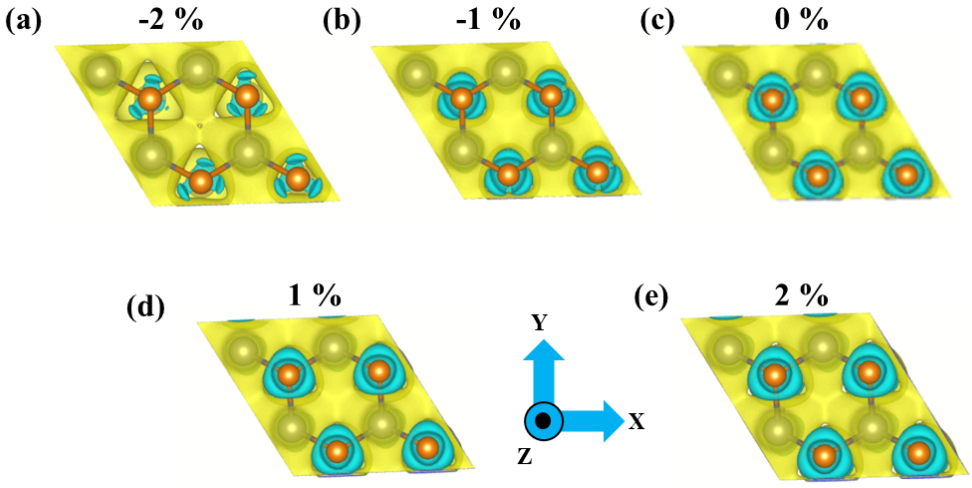

Fig. S3: Spin density, $\Delta\rho_s(\mathbf{r})$ of VSe_2/VN for (a) -2%, (b) -1%, (c) 0%, (d) $+1\%$, (e) $+2\%$, strain. Cyan and yellow represent negative spin density and positive spin density respectively.

In Figs. S3(a-e), the spin density, ($\Delta\rho_s(\mathbf{r}) = \rho_\uparrow(\mathbf{r}) - \rho_\downarrow(\mathbf{r})$) of the VSe_2/VN heterostructure evolves systematically with biaxial strain ($-2\% \rightarrow +2\%$). Here, we denoted the orange spheres as Se atoms, while V atoms were marked embedded in the positive spin density. Under compressive strain (-2% and -1%), the negative spin density around Se was weak; at zero strain, nearly symmetric cyan shells localized on Se, indicating stronger magnetic polarization. With tensile strain ($+1\%$ and $+2\%$), these cyan regions intensified and remained constant around Se. Overall, tensile strain enhanced and localized the negative spin density, whereas compressive strain suppressed and reduced localization.

S4. Orbital Projected Density of States (without SOC) of Spin-up and Spin-down Channels of VSe_2/VN Heterostructure

From the orbital projected density of states (PDOS) as depicted in Figs. S4(a-d), the metallic spin-up channel shows a clear finite density near E_F dominated by V1: d and V2: d states with the largest weight from V2: d_{z^2} and considerable contributions from d_{xy} and Se: p states (p_z and p_y) contributed appreciably and N was negligible. For the semiconducting spin-down channel, the valence band maximum was primarily V1: d and Se: p derived (notably d_{z^2}, $d_{x^2-y^2}$ of V1 with p_z and p_y of Se), whereas the conduction band minimum (just above E_F) was mainly V1: d like (led by d_{z^2} with some d_{zx} and d_{xy}), with little contribution of Se: p states (p_x and p_z) and no N contribution at either edge.

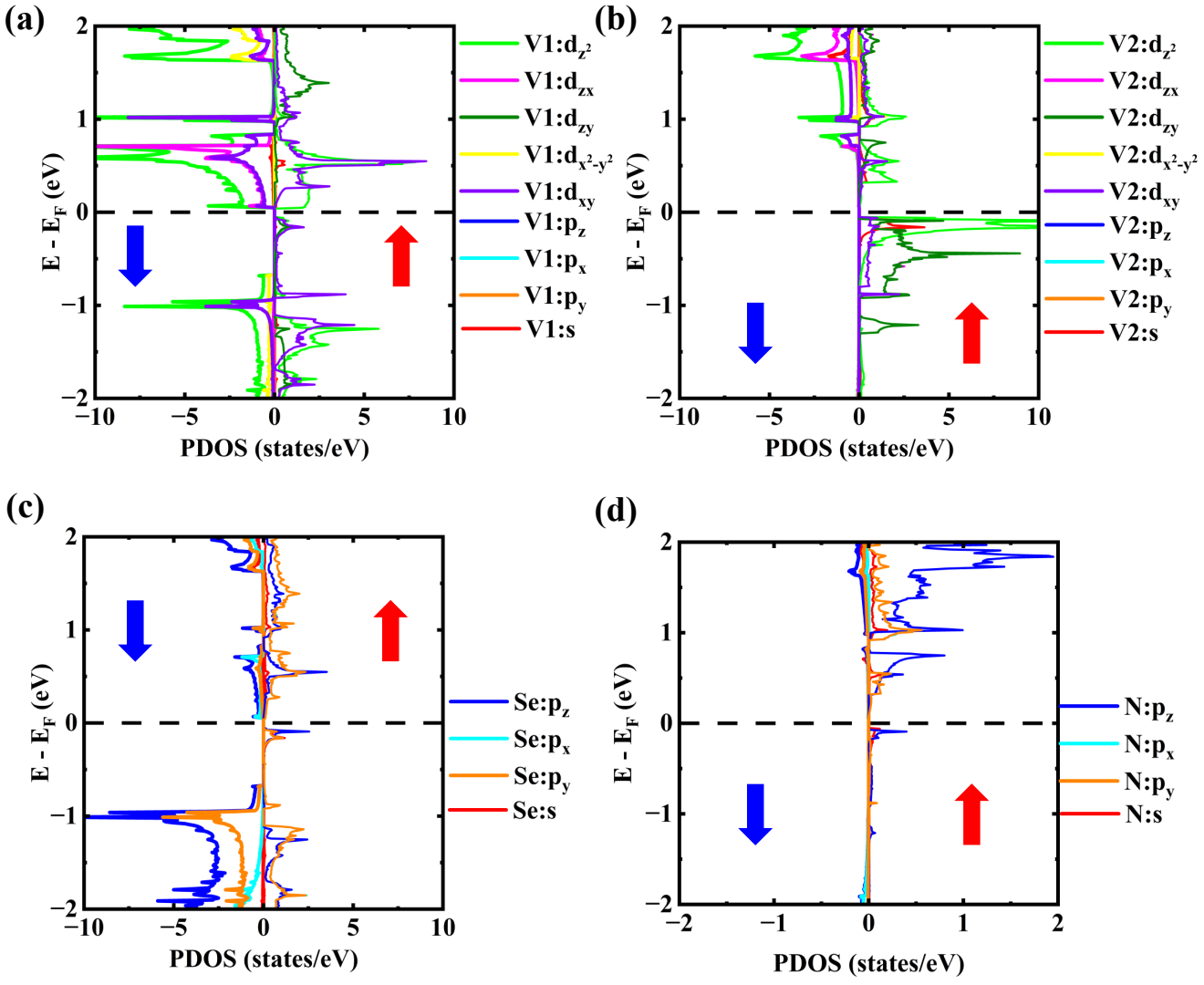

Fig. S4: Orbital PDOS of (a) V1 (V atom of VSe_2 of VSe_2/VN), (b) V2 (V atom of VN of VSe_2/VN), (c) Se, (d) N. Blue arrow represents spin-down channel and red arrow represents spin-up channel.

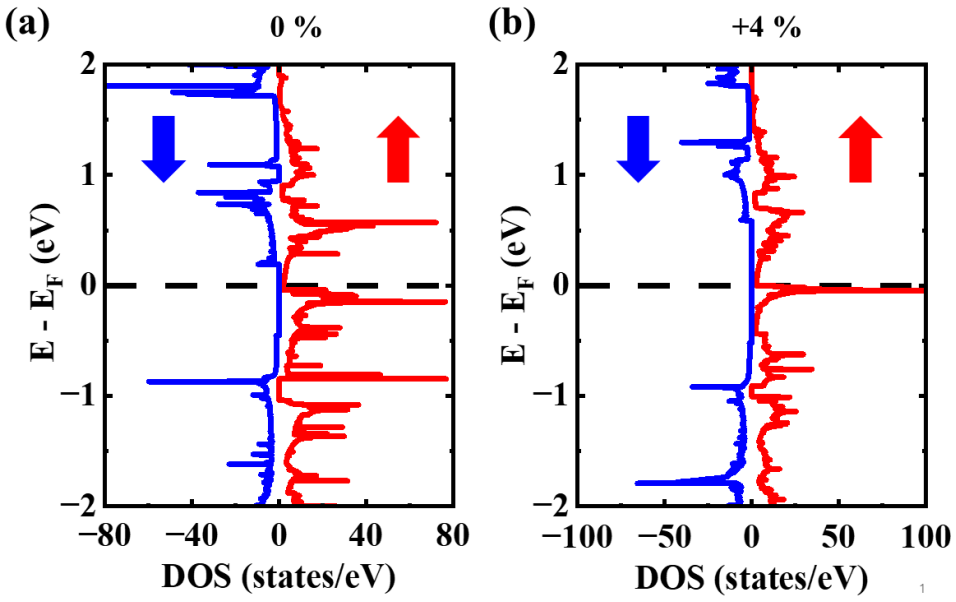

Fig. S5: Spin-polarized DOS at (a) 0% and (b) +4% strain. Blue arrow represents spin-down channel and red arrow represents spin-up channel.

S5. Effect of Tensile Strain in Spin-polarized Density of States of VSe_2/VN Heterostructure

Figs. S5(a) and (b) compare the spin-resolved DOS of VSe_2/VN at 0% and +4% strain where the horizontal dashed line marks the Fermi level E_F, blue arrow denotes the spin-down channel and red arrow denotes the spin-up channel. Within a narrow window around E_F (window $\Delta \to 0$), the spin-down DOS remained vanishing at both strains, indicating a clean gap at E_F for the spin-down channel. This directly explains the integrals in Eq. (S3): $n_\downarrow = \int_{E_F-\Delta}^{E_F} g_\downarrow(E)\, dE = 0$ at 0 K for both strain states.

By contrast, the spin-up DOS near E_F was considerable at 0% but strongly enhanced under +4% strain, with significant spectral weight appearing right at (and just below) E_F. Consistent with Eq. (S3), this produced a much larger spin-up occupation within the window: $n_\uparrow^{(0\%)} = 1.878455 \times 10^{-1}$ increased to $n_\uparrow^{(4\%)} = 1.574465$. Using the enhancement measure defined in Eq. (S4), $\mathcal{E}_\uparrow = n_\uparrow^{(4\%)}/n_\uparrow^{(0\%)} = 1.574465/0.1878455 \approx 8.38$; nearly a tenfold increment. Throughout, the system remained fully polarized in this energy window ($n_\downarrow = 0$). So, the strain primarily redistributed spin-up spectral weight towards E_F, reinforcing strain-tunable spin-filtering efficiency while preserving 100% polarization in the chosen window.

S6. Spin-up Concentration Enhancement of VSe_2/VN Heterostructure

The spin-resolved carrier concentrations were obtained from the spin-dependent DOS. For an energy window of half-width Δ centered at the Fermi energy E_F:

$$n_\uparrow = \int_{E_F-\Delta}^{E_F+\Delta} g_\uparrow(E)\, f(E)\, dE, \qquad n_\downarrow = \int_{E_F-\Delta}^{E_F+\Delta} g_\downarrow(E)\, f(E)\, dE \tag{S1}$$

where $n_\uparrow$ and $n_\downarrow$ are the spin-up and spin-down electron concentrations, $g_\uparrow(E)$ and $g_\downarrow(E)$ are the corresponding spin-resolved DOS, and $f(E)$ is the Fermi–Dirac distribution. Throughout this work, DOS were evaluated at 0 K, so we used $f(E)$ as a step function:

$$f(E) = \Theta(E_F - E) = \begin{cases} 1, & E \le E_F \\ 0, & E > E_F \end{cases} \tag{S2}$$

With Eq. (S2), only states below E_F contribute, and Eq. (S1) simplifies to

$$n_\uparrow = \int_{E_F-\Delta}^{E_F} g_\uparrow(E)\, dE, \qquad n_\downarrow = \int_{E_F-\Delta}^{E_F} g_\downarrow(E)\, dE \tag{S3}$$

From the DOS integrations within $[E_F - \Delta, E_F + \Delta]$ where $\Delta \to 0$, we obtained for the unstrained case (0% strain) $n_{\uparrow}^{(0\%)} = 1.878455 \times 10^{-1}$ and $n_{\downarrow}^{(0\%)} = 0$. Under 4% tensile strain, we found $n_{\uparrow}^{(4\%)} = 1.574465$ and $n_{\downarrow}^{(4\%)} = 0$. Thus, in this energy window at 0 K the system remained fully spin-polarized ($n_{\downarrow} = 0$), while the magnitude of the occupied spin-up states increased markedly with strain.

If enhancement, $\mathcal{E}$ is defined as the ratio of concentration at different strain levels of a particular spin,

$$\mathcal{E} = \frac{n_{\uparrow}^{(4\%)}}{n_{\uparrow}^{(0\%)}} \tag{S4}$$

this quantity is undefined for the spin-down channel as $n_{\downarrow}^{(0\%/4\%)} = 0$. Hence, we calculated enhancement for the spin-up channel,

$$\mathcal{E}_{\uparrow} = \frac{n_{\uparrow}^{(4\%)}}{n_{\uparrow}^{(0\%)}} = \frac{1.574465}{0.1878455} \approx 8.38$$

Hence, the occupied spin-up density near E_F showed an ~ 8.4 times increase; close to an order of magnitude.

S7. k-mesh Comparison for Sensitivity Check of Anomalous Hall Conductivity (AHC)

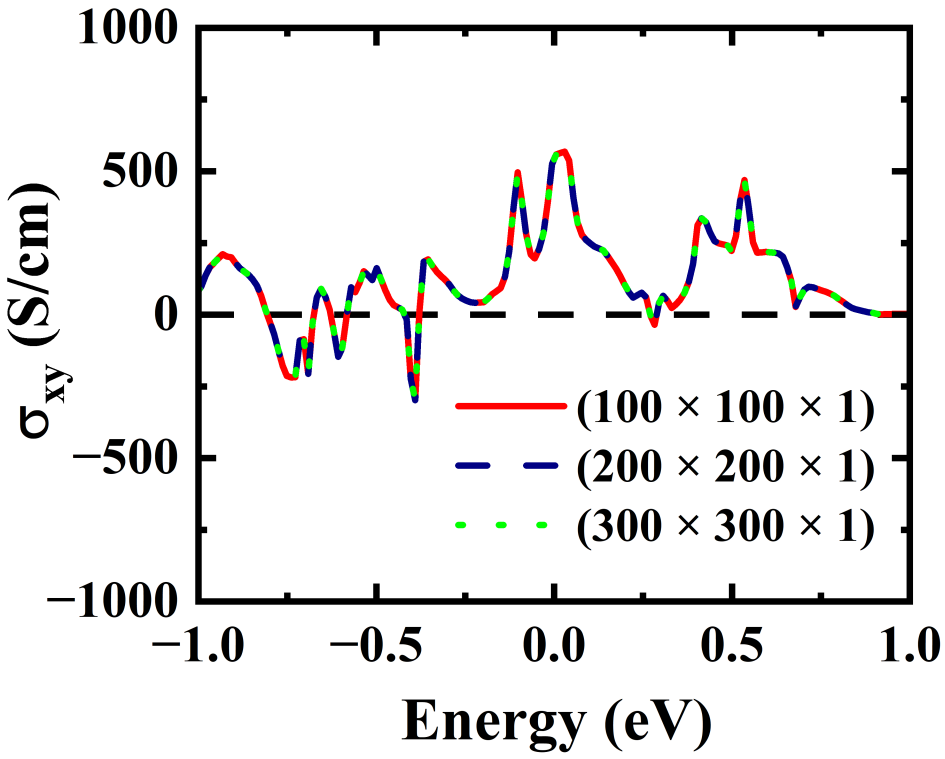

Fig. S6: Calculated anomalous Hall conductivity (σ_{xy}) as a function of energy for different k-meshes. The red solid line represents the $(100\times100\times1)$ k-mesh, the blue dashed line corresponds to the $(200\times200\times1)$ k-mesh, and the green dotted line corresponds to the $(300\times300\times1)$ k-mesh.

Fig. S6 illustrates the sensitivity test for AHC variation for different k-mesh including $(100 \times 100 \times 1)$, $(200 \times 200 \times 1)$, and $(300 \times 300 \times 1)$. The results are consistent across all k-mesh densities, indicating convergence of the calculation.

S8. Spin-polarized HSE06 Band Structure With SOC

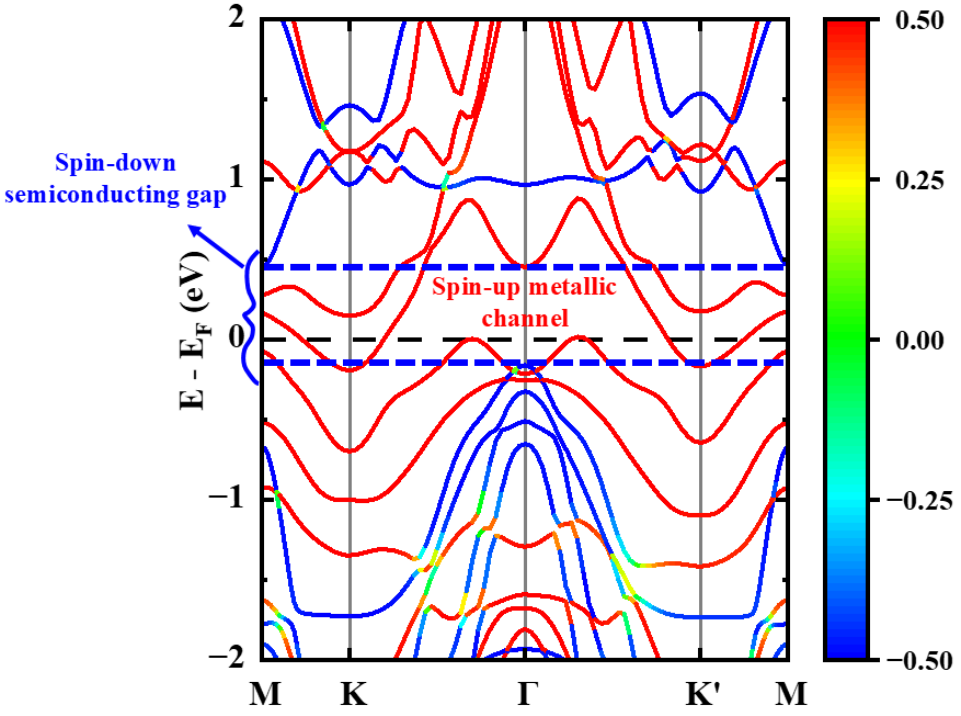

Fig. S7: Spin-polarized HSE06 band structure of unit cell with SOC, where spin-down channel (blue) shows semiconducting behavior and spin-up channel (red) shows metallic behavior. The color bar indicates expectation values of the spin operator on the spinor wave-functions ranging from -0.50 (blue) to +0.50 (red).

Fig. S7 depicts the half-metallic nature of VSe_2/VN heterostructure after considering HSE06 with SOC. Here, the spin-down channel (blue) clearly demonstrated a semiconducting nature, whereas the spin-up channel (red) showed a metallic nature.

S9. Zoomed Version of Spin-polarized Band Structure for Showing Valley Splittings

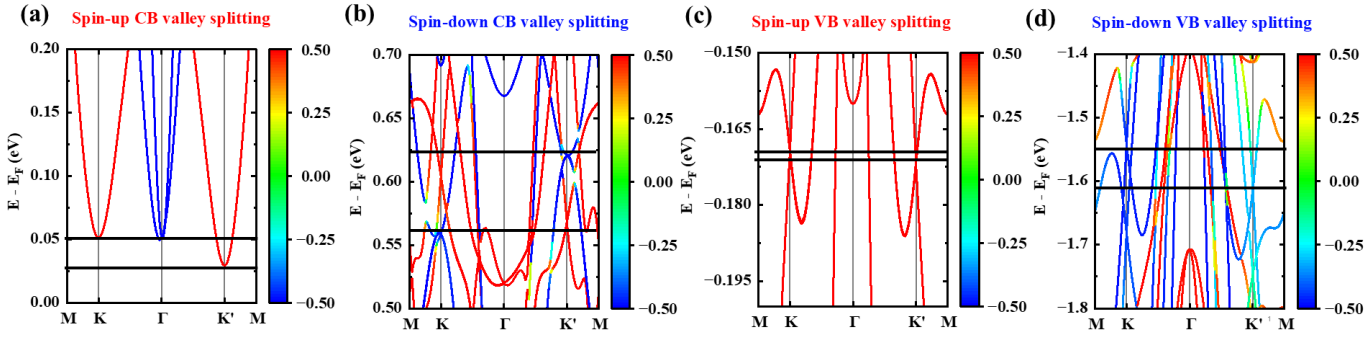

Fig. S8: CB valley splitting at K and K′, $\Delta C_{KK'}$ of (a) spin-up and (b) spin-down channels. VB valley splitting at K and K′, $\Delta V_{KK'}$ of (c) spin-up and (d) spin-down channels. The horizontal black lines indicate the valley splitting energy range.

Figs. S8(a-d) indicate the valley splittings (2×2×1) supercell at CB and VB at K and K′. For the unstrained case, $\Delta C_{KK'}$ of spin-up and spin-down channels are 22.9 meV and 61.3 meV, respectively. $\Delta V_{KK'}$ of spin-up and spin-down channels are 2.9 meV and 73.4 meV, respectively, for the same case.

References

[1] S. Feng, W. Mi, Strain and interlayer coupling tailored magnetic properties and valley splitting in layered ferrovalley 2H-VSe_2, Applied Surface Science 458 (2018) 191–197.

[2] A. Wasey, S. Chakrabarty, G. Das, Quantum size effects in layered VX_2 (X= S, Se) materials: Manifestation of metal to semimetal or semiconductor transition, Journal of Applied Physics 117 (2015).

[3] G. Hua, X. Wu, X. Ge, T. Zhou, Z. Shao, First-principles study on the high spin-polarized ferromagnetic semiconductor of vanadium-nitride monolayer and its heterostructures, Molecules 30 (2025) 2156.

[4] X. Bian, S. Lian, B. Fu, Y. An, Tunable spin-valley splitting and magnetic anisotropy of two-dimensional 2H-VS_2/h-VN heterostructure, Journal of Magnetism and Magnetic Materials 546 (2022) 168867.